ACS SENSORS

pubs.acs.org/acssensors Article

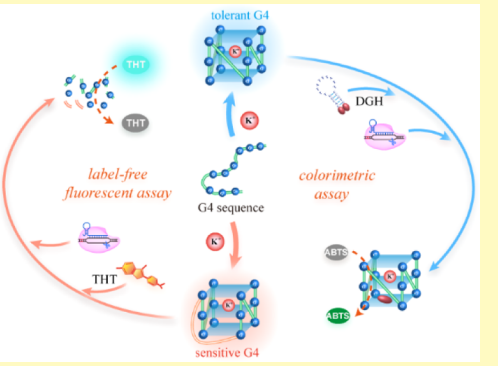
Pre-Folded G-Quadruplex as a Tunable Reporter to Facilitate CRISPR/Cas12a-Based Visual Nucleic Acid Diagnosis

Tiantian Yang, Juan Li,* Decai Zhang, Xiaoxue Cheng, Jia Li, Xiaolin Huang,* Shijia Ding, Ben Zhong Tang,* and Wei Cheng*

Cite This: https://doi.org/10.1021/acssensors.2c01391 Read Online

ACCESS | Metrics & More | Article Recommendations | Supporting Information

ABSTRACT: Clustered regularly interspaced short palindromic repeats (CRISPR)/Cas12a-based detection strategies with a fluorophore quencher-labeled ssDNA reporter or gold nanoparticle ssDNA reporter have been widely used in point-of-care (POC) molecular diagnostics. However, the potential of these CRISPR/Cas12a strategies for POC molecular diagnostics is often compromised due to the complex labeling, high cost, and low signal-to-noise ratio. Herein, we show a pre-folded G-quadruplex (G4) structure with tunable tolerance to CRISPR/Cas12a trans-cleavage and explore its mechanism. Two G4 structures (i.e., Tel22-10 and G16C) sensitive or tolerant to CRISPR/Cas12a trans-cleavage are designed and used as signal elements to fabricate a label-free visible fluorescent strategy or "signal-on" colorimetric strategy, respectively. These two strategies facilitate an ultrasensitive visual nucleic acid determination of Group B *Streptococci* with a naked-eye limit of detection of 1 aM. The feasibility of the developed G4-assisted CRISPR/Cas12a strategies for real-world applications is demonstrated in clinical vaginal/anal specimens and further verified by a commercial qPCR assay. This work suggests that the proposed G4 structures with tunable tolerance can act as promising signal reporters in the CRISPR/Cas12a system to enable ultrasensitive visible nucleic acid detection.



KEYWORDS: *G-quadruplex, CRISPR/Cas12a, label-free, signal-on, visual nucleic acid diagnosis*

Downloaded via SHANGHAI NORMAL UNIV on November 20, 2022 at 03:33:28 (UTC).
See https://pubs.acs.org/sharingguidelines for options on how to legitimately share published articles.

INTRODUCTION

Clustered regularly interspaced short palindromic repeats (CRISPR)/Cas12a-based visible nucleic acid detection has received increasing attention in the development of next-generation point-of-care (POC) molecular diagnostics technology owing to its trans-cleavage activity.[1−4] The main reason is that the trans-cleavage activity of Cas12a can convert target nucleic acid information into various visible signals. For example, upon recognition of double-stranded DNA (dsDNA) by the Cas12a-crRNA complex, Cas12 can indiscriminately cleave a quenched-fluorescent single-stranded DNA (ssDNA) reporter or gold nanoparticle ssDNA reporter, releasing the fluorescence dye to yield a visible fluorescent signal or the gold nanoparticles to yield a visible colorimetric signal.[5−7] Nevertheless, the application of the conventional CRISPR/Cas12a system for POC testing is often compromised due to the complex labeling and high cost of double-labeled quenched-fluorescent ssDNA and low signal-to-noise ratio of the gold nanoparticle ssDNA reporter. Therefore, developing a signal element with a label-free visible fluorescent reporter and a low colorimetric background reporter for POC testing applications of CRISPR/Cas12a-based visual nucleic acid diagnosis is urgently needed.

Guanine quadruplexes (G4s) are the most studied non-canonical DNA secondary structures, consisting of stacked G-quartets via Hoogsteen hydrogen-bonding assembly.[8,9] Owing to their special advantages of easy synthesis, small size, low cost, and great thermal stability, G4s have attracted increasing interest in the design and development of highly sensitive molecular diagnostic elements.[10−13] Currently, G4-based visual nucleic acid detection probes mainly involve a fluorescence signal and a colorimetric signal. For example, upon integration of specific ligands (Thioflavin T, ThT) by G4s, the G4 complex can produce a strong fluorescence signal and can be used as a label-free fluorescent probe.[14−17] Moreover, the G4-based signal element can be used as a catalytic colorimetric probe when G4 binds hemin and triggers its peroxidase-like activity.[18−21] The robust multifunctional signal output property of G4s makes them an ideal signal readout candidate for visual biosensors.

Combining the CRISPR/Cas12a system with G4 signal elements is in favor of developing highly sensitive methods. Liu et al. first proposed that G4 sequences could be cleaved by

Received: June 30, 2022
Accepted: November 9, 2022

© XXXX American Chemical Society

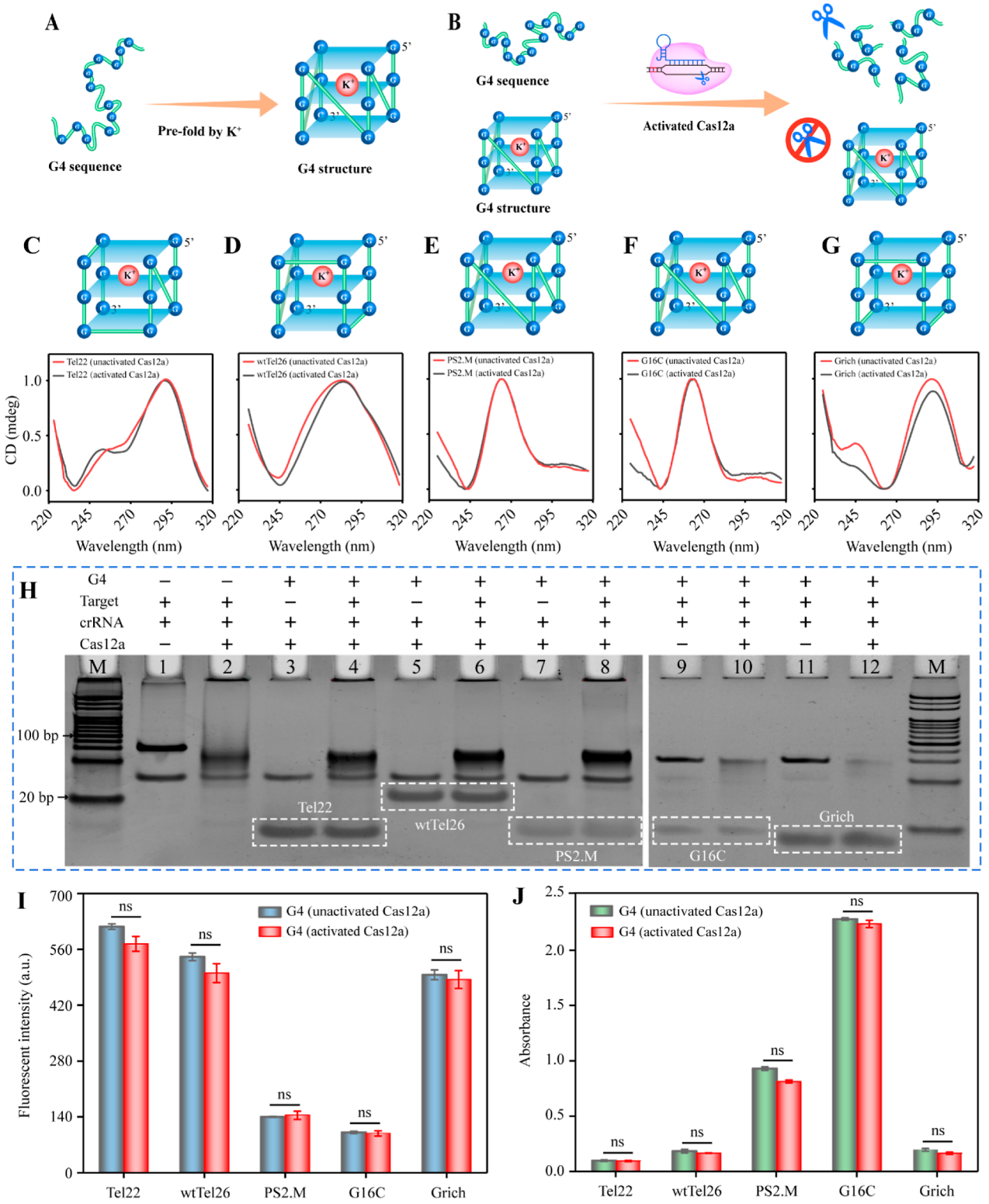


Figure 1. Design of the pre-folded G4 structure and characterization of tolerance to Cas12a. (A) Synthetic strategy of G4 structures. (B) Schematic illustration for the comparison of tolerance of raw G4 sequence and K^+ pre-folded G4 structures in the activated Cas12a system. (C−G) CD spectra of K^+ pre-folded G4 structures (5 μM) after incubation with unactivated Cas12a and activated Cas12a (250 nM). (H) PAGE of K^+ pre-folded G4 structures (5 μM) after incubation with unactivated Cas12a and activated Cas12a (250 nM). (I) Fluorescence intensity (487 nm) of well-folded G4 structures/ThT complex after incubation with unactivated Cas12a and activated Cas12a. (J) Absorbance (414 nm) of ABTS catalyzed by the well-folded G4 structures/hemin complex after incubation with unactivated Cas12a and activated Cas12a. Error bars obtained from three independent experiments. An unpaired Student's t-test was used to assess statistical significance, "ns" means no significance.

Cas12a,[22] and then Xu et al. designed colorimetric strategies based on the G4 sequence trans-cleaved by Cas12a.[23,24] However, these colorimetric strategies are "signal-off" and show a non-specific fold of G4 structures, which affects the

https://doi.org/10.1021/acssensors.2c01391
ACS Sens. XXXX, XXX, XXX−XXX

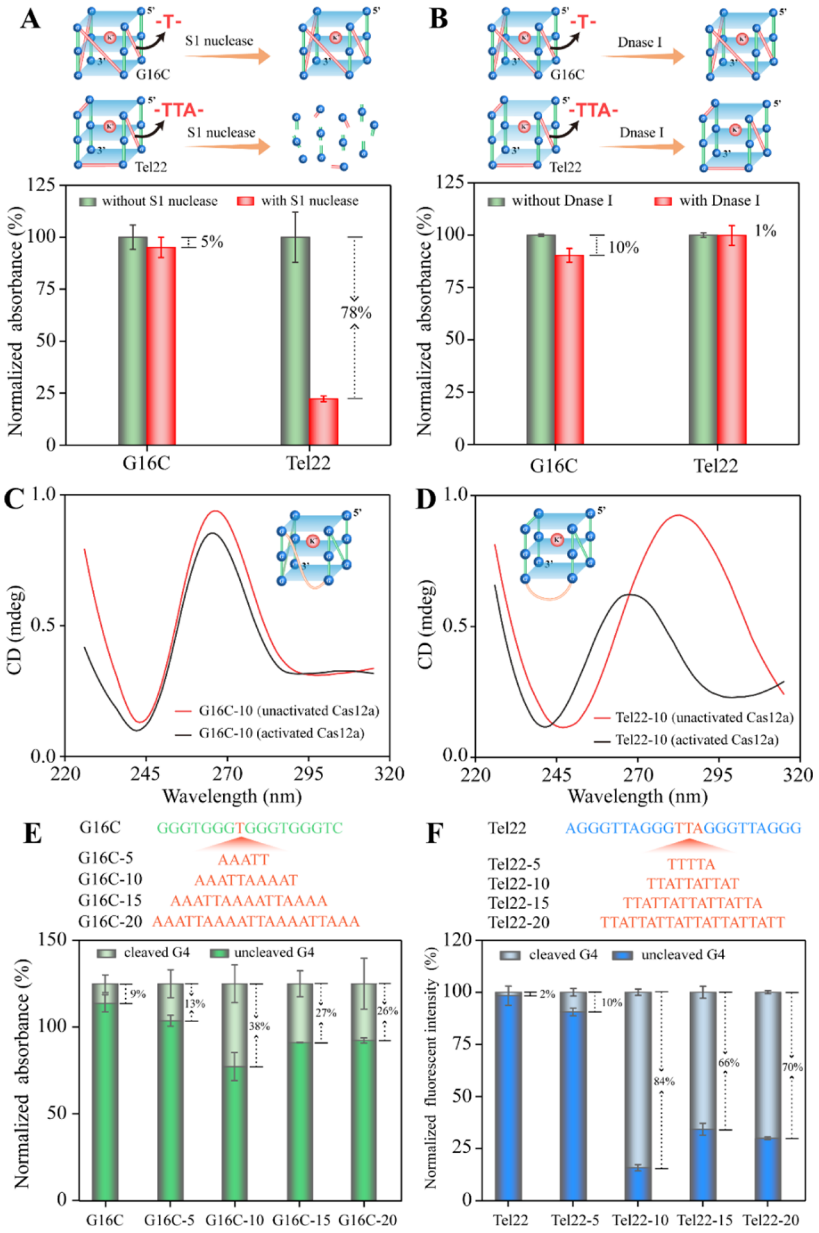


Figure 2. Investigation of the tolerance mechanism of well-folded G4 structures to CRISPR/Cas12a. (A,B) Absorbance (414 nm) of ABTS catalyzed by the G16C/hemin and Tel22/hemin complexes after incubation with S1 nuclease and DNase I, respectively. The concentration of both S1 nuclease and DNase I was 80 U/mL and that of G4 structures was 250 nM. (C,D) CD spectra of G16C-10 and Tel22-10 after incubation with unactivated Cas12a and activated Cas12a (250 nM). Inset: structural diagram of G16C-10 and Tel22-10, respectively. The concentration of both G16C-10 and Tel22-10 was 5 μM. (E) Absorbance (414 nm) of ABTS catalyzed by the G16C/hemin complex with various loop lengths of G16C after incubation with unactivated Cas12a and activated Cas12a. (F) Fluorescence intensity (487 nm) of the Tel22/ThT complex with various loop lengths of Tel22 after incubation with unactivated Cas12a and activated Cas12a. Ratio (%) represents the percentage of digested G4s in whole G4s. Error bars obtained from three independent experiments.

cleavage efficiency. To eliminate the background signal and improve the sensitivity, Wang et al. developed a new Cas12a-assisted G4/hemin strategy by cleaving the antisense sequence of G4 for visual *Bacillus anthracis* analysis with a LOD of as low as one copy.[25] However, this method depends on the high-temperature denaturation and annealing process of G4 and antisense G4, which limits its application in the POC molecular diagnostics. Therefore, how to achieve a simple "signal-on" colorimetric strategy by integrating the CRISPR/Cas12a system with the G4 signal element to eliminate the background signal remains huge challenges. In addition, there is still a need for the design of a G4-based label-free visible fluorescent strategy that can avoid self-assembly of the G4 sequence in the CRISPR/Cas12a reaction buffer.[26]

In this work, we first proposed pre-folded G4 structures to fabricate multifunctional signal elements and demonstrate their potential for developing a simple label-free visible fluorescent strategy and a "signal-on" colorimetric strategy in the CRISPR/Cas12a-based POC testing system. The G4 structures were pre-prepared by employing potassium ion (K^+) as a stabilizer to form a well-folded G4 structure. Through systematically regulating the loop length of the well-folded G4 structure, the tolerance of the G4 structure to CRISPR/Cas12a could be adjusted. After being integrated with the CRISPR/Cas12a

https://doi.org/10.1021/acssensors.2c01391
ACS Sens. XXXX, XXX, XXX−XXX

system, the well-folded G4 structure (i.e., Tel22-10 and G16C) with different tolerances could be used as the label-free visible fluorescent signal element and "signal-on" colorimetric signal element. After optimization, the developed two strategies could detect the Group B *Streptococci* (GBS)-specific DNA fragment with a naked-eye LOD of 1 aM. Moreover, the sensitivity and specificity of the two strategies to detect GBS in clinical vaginal/anal samples of pregnant women achieved 100%. Overall, this work demonstrates a designed strategy using a well-folded G4 structure as a multifunctional signal element for the development of ultrasensitive visual POC molecular diagnostics technology based on CRISPR/Cas12a.

RESULTS AND DISCUSSION

Design of the Pre-Folded G4 Structure and Adjustment of Tolerance to Cas12a. Figure 1A depicts the synthetic strategy of G4 structures. Various G4 sequences (Tel22, wtTel26, PS2.M, G16C, and Grich) were selected as the model.[27−30] The well-folded G4 structure stabilized by K^+ was synthesized using a thermal annealing method in accordance with a previous report.[31] Circular dichroism (CD) spectroscopy (Figure 1C−G, red line) showed that the pre-folded Tel22, wtTel26, PS2.M, G16C, and Grich sequences displayed the typical spectral features of hybrid-stranded, parallel-stranded, and antiparallel-stranded conformation,[32] indicating that these G4 sequences were folded into stable G4 structures when they were premixed with K^+.

To examine the tolerance of these well-folded G4 structures, activated Cas12a was added to cleave the G4 structures. The results in Figure 1C−G (black line) showed that no obvious spectral changes were observed in all well-folded G4 structures compared with their original CD spectra, demonstrating that the activated Cas12a did not cleave the well-folded G4 structures (Figure 1B). The tolerance of well-folded G4 structures was further confirmed by the polyacrylamide gel electrophoresis (PAGE) assay. The results in Figure 1H showed that the migration and intensity of the bands of well-folded G4 structures were unaffected by the Cas12a cleavage (Figure S1), indicating that the pre-folded G4 structures could maintain the structural integrity even in the presence of the Cas12a cleavage. Notably, Tel22, wtTel26, PS2.M, G16C, and Grich sequences could be completely cleaved by activated Cas12a (Figure S2). The integrity of these G4 structures was further investigated by ligand binding assays. Considering the significant increase of fluorescence intensity and peroxidase-like catalytic activity after G4 structures combined with ThT and hemin, they were selected as fluorescent and colorimetric ligands, respectively. Figure 1I shows that the fluorescence intensity at 487 nm of well-folded G4 structures/ThT complex did not change after incubation with the activated Cas12a. A similar result in absorbance at 414 nm was observed by using the well-folded G4 structures/hemin complex to catalyze 2,2′-azinobis-(3-ethylbenzthiazoline-6-sulfonate) (ABTS) (Figure 1J). However, remarkable reduction of fluorescence and colorimetric signals was observed when directly the raw G4 sequences and activated Cas12a were mixed (Figure S3), which is probably because the raw G4 sequences could be quickly cleaved by activated Cas12a before folded stabilized G4 structures in the reaction buffer (Figure S4). The above results verified that the pre-folded G4 structure stabilized by K^+ could tolerate the trans-cleavage of CRISPR/Cas12a.

Considering that K^+ is crucial to improve the tolerance of G4 structures, we evaluated the effect of the K^+ concentration on the tolerance of G4 structures. Tel22 and G16C were selected as the model because they have the highest binding capacity to ThT and hemin (Figure 1I,J), respectively. The results showed that the tolerance of Tel22 and G16C to CRISPR/Cas12a trans-cleavage increased gradually with increasing K^+ concentration from 0 to 100 mM and reached a plateau at 200 mM (Figure S5). In addition, the G4 structures (formed by Tel22 and G16C) stabilized with 100 mM K^+ also remained intact after incubation with activated Cas12a for 120 min (Figure S6). These results demonstrated that the G4 sequences pre-folded by 100 mM K^+ can form stable G4 structures and exhibit high tolerance to the trans-cleavage of CRISPR/Cas12a.

To specify the tolerance mechanism of well-folded G4 structures to CRISPR/Cas12a, the different endonucleases were used to cleave the well-stabilized G4 structures. S1 nuclease[33] and DNase I[34] were selected as the ideal endonucleases, and the G16C/hemin and Tel22/hemin catalyze ABTS as the signal output. For the cleavage of the S1 nuclease, the absorbance of the G16C/hemin system and Tel22/hemin system decreased by 5 and 78% (Figure 2A), respectively, indicating that the S1 nuclease could cleave Tel22 but not G16C. This is probably because G16C has one nucleotide in its loop structure, while Tel22 has three nucleotides, thus providing more suitable sites for the cleavage of the S1 nuclease (cleavage of the ssDNA into a single oligonucleotide).[35] For the cleavage of DNase I, the absorbance of the G16C/hemin system and Tel22/hemin system changed slightly (10 and 1%) (Figure 2B), which was consistent with the CRISPR/Cas12a system (Figure S7), indicating that DNase I could not cleave Tel22 and G16C. The possible reason was that Tel22 and G16C do not provide suitable sites for the cleavage of DNase I and the CRISPR/Cas12a system [cleavage of the ssDNA into longer oligonucleotides (4 nt)].[34,36]

To confirm that the loop of G4 structures is a possible site affecting its tolerance to the CRISPR/Cas12a system, we further added 10 nucleotides of thymine/guanine on the middle loop of G16C (G16C-10) and Tel22 (Tel22-10) (Figure 2C,D), respectively. The results showed that the typical CD spectra of G16C-10 and Tel22-10 significantly changed, demonstrating that the activated Cas12a can cleave the well-folded G16C-10 and Tel22-10. The cleavage of G16C-10 and Tel22-10 by activated Cas12a was further verified by the PAGE assay and ligand binding assays (Figures S8−S10). These data indicated that the tolerance of G4 structures to CRISPR/Cas12a trans-cleavage was related to the loop length of G4 structures.

To clarify the effect of different loop lengths on the cleavage efficiency, we added 5, 10, 15, and 20 nucleotides of thymine/guanine on the middle loop of G16C (named G16C-5 to 20; Figure 2E) and Tel22 (named Tel22-5 to 20; Figure 2F), respectively. First, G16C/hemin-catalyzed ABTS was used as the signal output to verify the cleavage efficiency of G16C. The results showed that the cleavage efficiency gradually increased from 9 to 38% as nucleotides increased from 0 to 10 and then decreased with the continuous increase of nucleotides (Figure 2E), demonstrating that G16C and G16C-10 had high and low tolerance to CRISPR/Cas12a trans-cleavage, respectively. Second, the Tel22/ThT system was used as the signal output to verify the cleavage efficiency of Tel22. Results showed that the cleavage efficiency gradually increased from 2 to 84% as nucleotides increased from 0 to 10 and then decreased with the

https://doi.org/10.1021/acssensors.2c01391
ACS Sens. XXXX, XXX, XXX−XXX

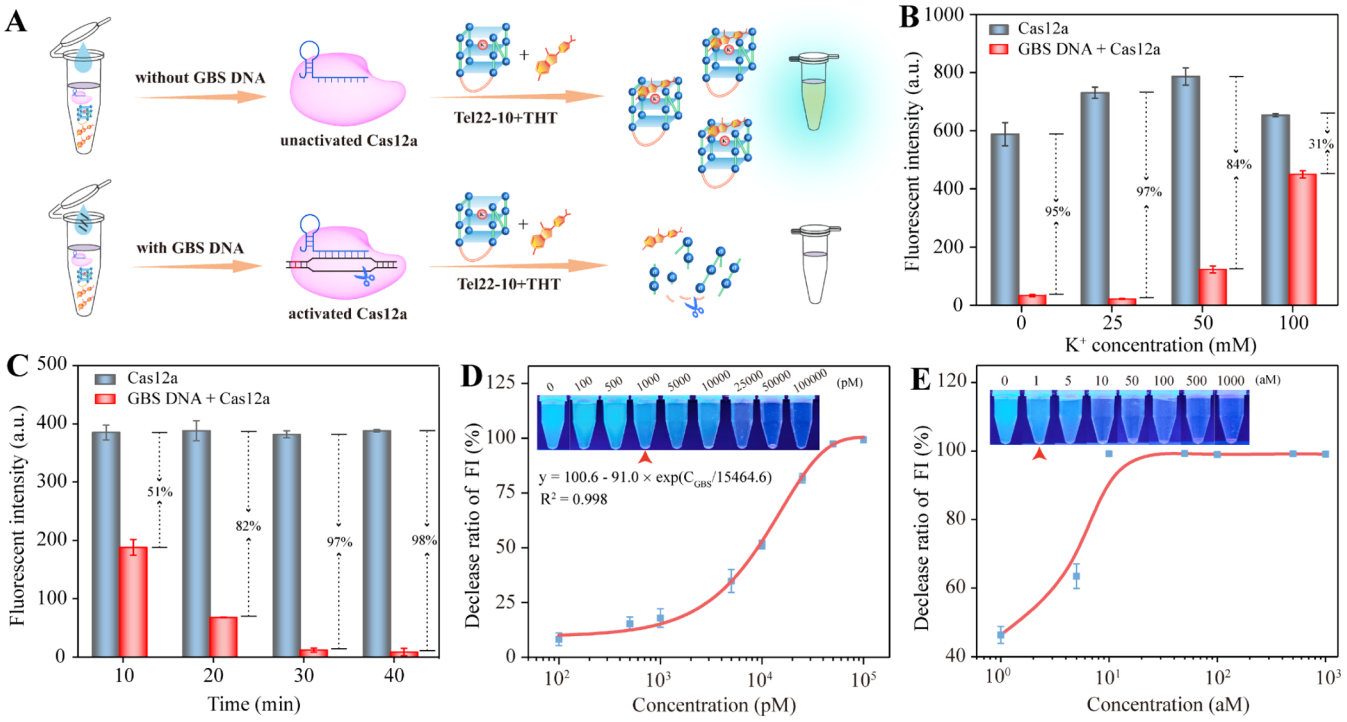


Figure 3. Analytical performance of the CRISPR/Cas12a-Tel22-10/ThT system for GBS DNA detection. (A) Schematic representation of the label-free visible fluorescent strategy for the detection of GBS DNA. (B) Fluorescence intensity of ThT in the Tel22-10 structure stabilized by various concentrations of K^+ before and after adding GBS DNA-activated Cas12a. The GBS DNA concentration was 100 nM. (C) Fluorescence intensity of ThT in Tel22-10 structures (stabilized by 25 mM K^+) under different incubation times before and after adding GBS DNA-activated Cas12a. (D) Calibration curve between the decreased ratio of fluorescence intensity at 487 nm and the GBS DNA concentration in a range of 10^2 to 10^5 pM. Inset: photographs of the CRISPR/Cas12a-Tel22-10/ThT system in response to different concentrations of GBS DNA. (E) Calibration curve between the decreased ratio of fluorescence intensity at 487 nm and GBS DNA amplified RPA technology (10^0 to 10^3 aM). Inset: photographs of the RPA-assisted CRISPR/Cas12a-Tel22-10/ThT system in response to different concentrations of GBS DNA.

continuous increase of nucleotides (Figure 2F), demonstrating that Tel22 and Tel22-10 had high tolerance and sensitivity to CRISPR/Cas12a trans-cleavage, respectively. The reason is that the long loop (>10 nt) sequence is far away from the G-core region, increasing the recognition probability of Cas12a and also increasing the difficulty of folding the G-core region, thereby affecting the stability of the G4 structure. These results confirmed that the well-folded Tel22/G16C could tolerate the trans-cleavage of CRISPR/Cas12a, and this tolerance to CRISPR/Cas12a trans-cleavage is tunable by simply increasing the loop length. In short, the pre-folded G4 structure provides a promising alternative to the fabrication of multifunctional signal elements by manipulating the anti-CRISPR/Cas12a trans-cleavage activity of G4s.

CRISPR/Cas12a Trans-Cleavage-Sensitive Tel22-10 as a Label-Free Visible Fluorescent Signal Element. Owing to its high sensitivity to the CRISPR/Cas12a trans-cleavage, Tel22-10 was used as a label-free visible fluorescent signal element in the CRISPR/Cas12a system to facilitate visual nucleic acid diagnosis of GBS, an important indicator for the maternal and newborn infection.[37] Figure 3A depicts the testing principle of the designed CRISPR/Cas12a-Tel22-10/ThT system for the ultrasensitive detection of GBS DNA. The system design relies on the combination of Tel22-10 and ThT to produce a strong fluorescence signal. In the presence of GBS, the target DNA was first integrated into Cas12a to form the activated Cas12a. Activated Cas12a then rapidly cleaved Tel22-10 and destroyed its secondary structure. Through collateral cleavage, the fluorescence intensity decreased dramatically. On the contrary, Cas12a could not be activated, and the fluorescence intensity did not change.

The optimization of reaction conditions is the key to improve the detection performance of this CRISPR/Cas12a-Tel22-10/ThT system. Here, several important parameters, including K^+ concentration for stabilizing the Tel22-10 structure and collateral cleavage time of activated Cas12a before readout, were evaluated. As shown in Figure 3B, the decrease rate of fluorescence intensity first increased from 95 to 97% with the increase of K^+ concentration from 0 to 25 mM and then decreased to 31% with the continuous increase of K^+ concentration, indicating that the optimal K^+ concentration for stabilizing was 25 mM. For optimizing the collateral cleavage time, the decrease rate of fluorescence intensity gradually increased from 51 to 97% with the increase of reaction time from 10 to 30 min and then reached a balance upon prolonging the reaction time further (Figure 3C). In addition, appropriate K^+ concentration in the reaction buffer is crucial to ensure the Cas12a trans-cleavage activity. If there was no K^+ in reaction buffer, the trans-cleavage efficiency of Cas12a was significantly decreased, which is not conducive to the decrease of more than 90% signal intensity (Figure S11). These results indicated that 30 min of collateral cleavage time was enough to enable the complete destruction of the Tel22-10 structure for obtaining the best analytical performance, which was superior to that of the fluorophore quencher-labeled ssDNA reporter for GBS DNA detection (Figure S12). The possible reason was that the Tel22-10 structures increase the recognition probability of Cas12a.

https://doi.org/10.1021/acssensors.2c01391
ACS Sens. XXXX, XXX, XXX−XXX

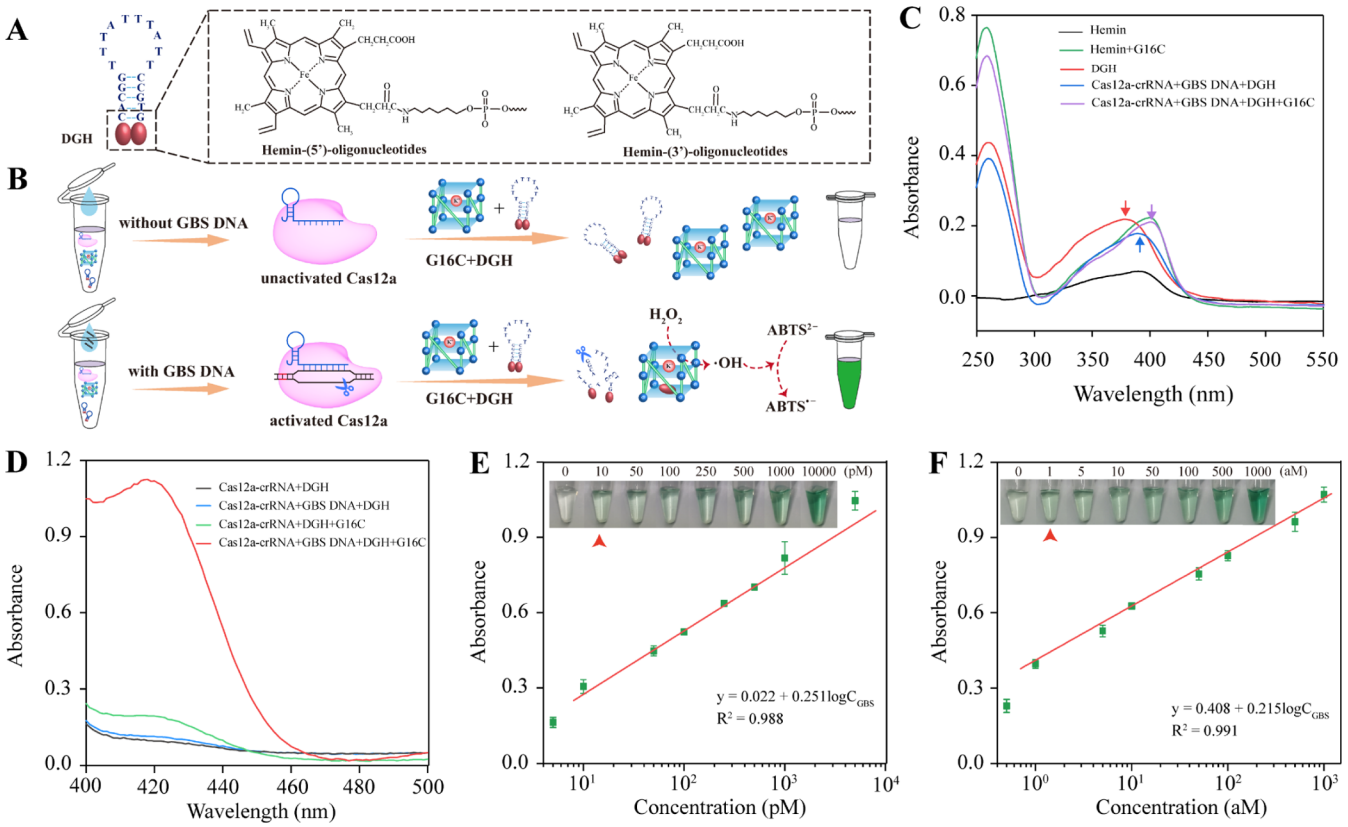


Figure 4. Analytical performance of the CRISPR/Cas12a-G16C/hemin system for GBS DNA detection. (A) Structural diagram of DGH. (B) Schematic representation of the "signal-on" colorimetric strategy for the detection of GBS DNA. (C) UV−vis spectra of hemin (2 μM); the mixture of hemin (2 μM) and G16C (2 μM); DGH (1 μM); the mixture of DGH (1 μM), Cas12a-crRNA (100 nM), and GBS DNA (100 nM); and the mixture of DGH (1 μM), G16C (2 μM), Cas12a-crRNA (100 nM), and GBS DNA (100 nM). (D) UV−vis spectra of ABTS (2 mM) catalyzed by the mixture of Cas12a-crRNA and DGH; the mixture of Cas12a-crRNA, GBS DNA, and DGH; the mixture of Cas12a-crRNA, G16C, and DGH; and the mixture of Cas12a-crRNA, GBS DNA, G16C, and DGH. The concentrations of Cas12a-crRNA, GBS DNA, DGH, and G16C were 50, 100, 150, and 450 nM, respectively. (E) Calibration curve between the absorbance at 414 nm and the GBS DNA concentration in a range of 0−10^4 pM. Inset: photographs of the CRISPR/Cas12a-G16C/hemin system in response to different concentrations of GBS DNA. (F) Calibration curve between the absorbance at 414 nm and GBS DNA amplified RPA technology (0−10^3 aM). Inset: photographs of the RPA-assisted CRISPR/Cas12a-G16C/hemin system in response to different concentrations of GBS DNA.

Under the developed conditions, GBS DNA solutions with various concentrations (0−10^5 pM) were monitored using the CRISPR/Cas12a-Tel22-10/ThT system. The detection results were recorded using a fluorescence spectrophotometer and mobile phone. The LOD was defined as the lowest concentration of GBS DNA to produce the fluorescence signal recorded by the reader. As shown in the inset of Figure 3D, the fluorescence of the reaction solution gradually diminished with increasing GBS DNA concentration, and the LOD observed by the naked eye was 1 nM. Figure 3D shows a good correlation between the decreased ratio of fluorescence intensity (FI) at 487 nm and the GBS DNA concentration from 0 to 10^5 pM, and the corresponding regression equation was described as $y = 100.6-91.0 \times \exp(C_{GBS}/15464.6)$ ($R^2 = 0.998$). The LOD obtained by the fluorescence spectrophotometer was 100 pM, which was comparable to that of the fluorophore quencher-labeled ssDNA reporter for GBS DNA detection (Figure S13).

To further improve the detection sensitivity, recombinase polymerase amplification (RPA) was introduced to pre-amplify the GBS DNA fragment for 30 min. As shown in the inset of Figure 3E, the fluorescence of the reaction solution weakened gradually and even disappeared with increasing GBS DNA concentration. An apparent decrease in fluorescence could be observed when the DNA concentration was 1 aM, indicating that the LOD obtained by the naked eye was as low as 1 aM. Additionally, similar results were obtained by the fluorescence spectrophotometer, and the LOD was also 1 aM. Furthermore, the specificity of the label-free visible fluorescent strategy was evaluated by the detection of the GBS strain and the non-GBS strains (*Streptococcus pneumoniae*, *Escherichia coli*, Group A *Streptococcus*, *Staphylococcus aureus*). As indicated in Figure S14, we can observe an evident signal response toward GBS compared with that toward other non-GBS strains, implying high selectivity of the proposed fluorescent strategy for specifically distinguishing GBS against other nontargets. The results suggested that the developed label-free visible fluorescent signal output element based on Tel22-10/ThT can be used as a promising alternative to the traditional fluorophore quencher-labeled ssDNA reporter, avoiding complex double labeling and reducing the testing cost.

CRISPR/Cas12a Trans-Cleavage-Tolerant G16C as a "Signal-On" Colorimetric Signal Element. The "signal-on" colorimetric strategy with low color background is crucial to improve the detection sensitivity of the CRISPR/Cas12a-based colorimetric system. Considering its high tolerance to CRISPR/Cas12a trans-cleavage, G16C was used as a "signal-on" colorimetric signal element in the CRISPR/Cas12a system to facilitate visual nucleic acid diagnosis. To achieve a "signal-

https://doi.org/10.1021/acssensors.2c01391
ACS Sens. XXXX, XXX, XXX−XXX

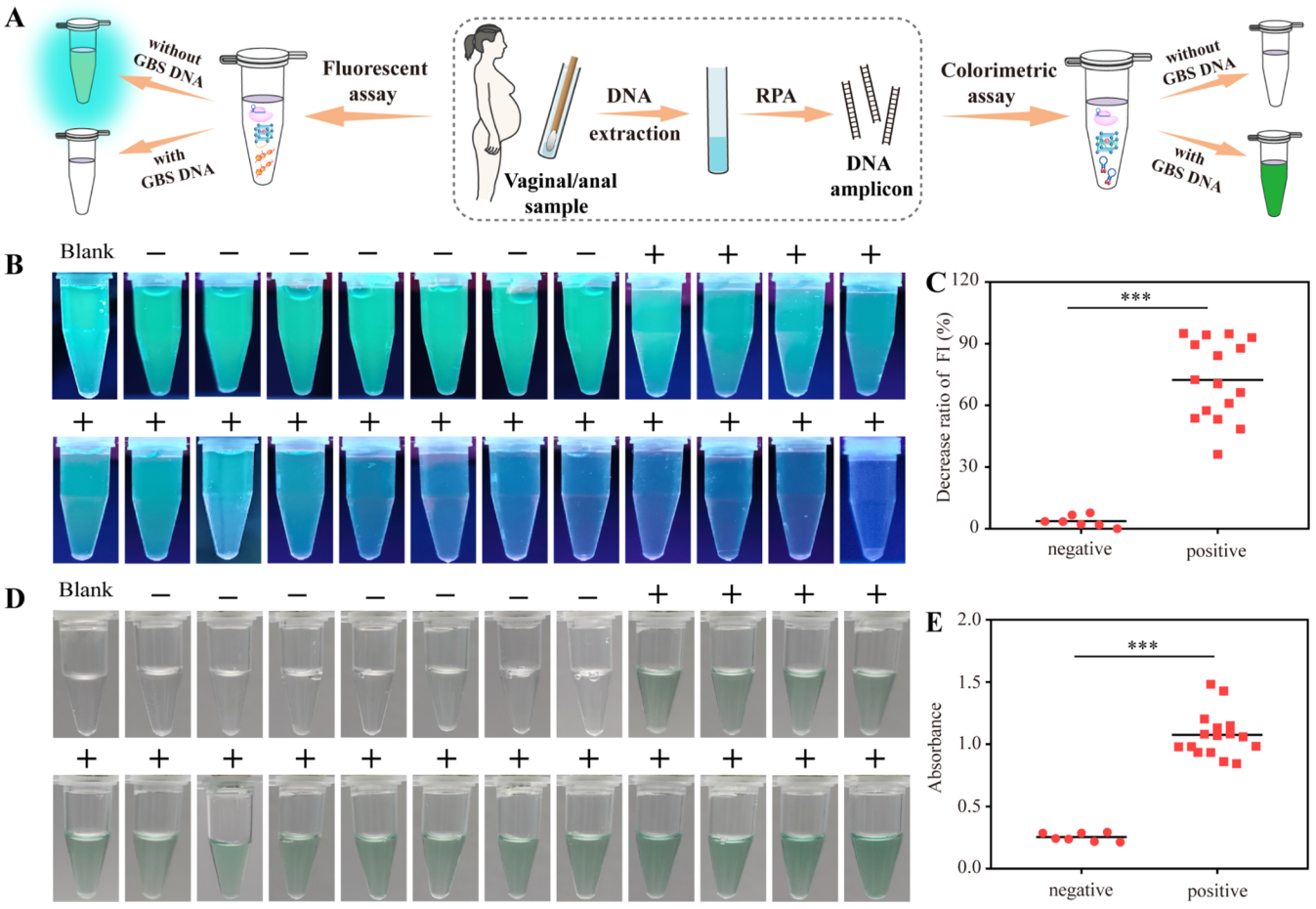


Figure 5. Application of the label-free visible fluorescent strategy and "signal-on" colorimetric strategy in the diagnosis of GBS infection in pregnant women. (A) Schematic diagram of two strategies for the detection of GBS in clinical vaginal/anal samples of pregnant women. (B) Photographs of GBS in clinical vaginal/anal samples of pregnant women detected by a label-free visible fluorescent strategy. (D) Photographs of GBS in clinical vaginal/anal samples of pregnant women detected by a "signal-on" colorimetric strategy. (C) Scatter plot of the decreased ratio of fluorescence intensity (487 nm) of 23 vaginal/anal samples detected by a fluorescent strategy. The 10% reduction in fluorescence intensity was defined as a positive threshold. (E) Scatter plot of the absorbance (414 nm) of 23 vaginal/anal samples detected by a colorimetric strategy. The absorbance greater than 0.3 was defined as a positive threshold. "−" and "+" represent the negative and positive samples, respectively. "Blank" indicated the result of using two strategies to detect the extraction solution of commercial kit. An unpaired Student's *t*-test was used to assess statistical significance of two groups; "***" means $p < 0.001$.

on" strategy, the DNA-grafted hemin dimer (DGH) probes were designed and introduced into the detection system (Figure 4A). The developed DGH probes can inhibit the catalytic activity of hemin monomers by grafting two hemin molecules to two terminals of an oligonucleotide.[38,39] Figure 4B depicts the testing principle of the designed CRISPR/Cas12a-G16C/hemin system for the ultrasensitive detection of GBS DNA. In the presence of GBS DNA, the target DNA was first integrated into Cas12a to form the activated Cas12a. The activated Cas12a then rapidly cleaved the loop sequence of DGH and released the hemin monomers. Then, the released hemin monomers quickly bound to the well-stabilized G16C structures (uncleaved by activated Cas12a) to form active G16C/hemin DNAzymes, which can catalyze ABTS to generate a green-colored signal. On the contrary, Cas12a could not be activated, and the color of the reaction solution exhibited negligible change (colorless).

To verify the feasibility of the "signal-on" colorimetric strategy, the DGH probes were first characterized by a UV−vis spectrophotometer. As shown in Figure 4C, compared with the free hemin monomers (black line), the absorption peak of DGH probes (red line) shifted from 394 to 378 nm.[38,40] After adding activated Cas12a, the DGH probes (blue line) showed a similar absorption peak to that of free hemin monomers (black line), indicating that the designed DGH probes could be cleaved by activated Cas12a. With the addition of the well-folded G16C, the released hemin monomers from the DGH probes can bind with the well-folded G16C to form the G16C/hemin complex, which was confirmed by the absorption peak shift from 394 to 402 nm,[40] similar to the directly assembled G16C/hemin DNAzymes. The catalytic activity of the formed G16C/hemin DNAzymes was further evaluated. Figure 4D shows that the absorbance significantly increased when the DGH probes, activated Cas12a, and well-folded G16C were mixed. The uncleaved DGH probes can also generate a negligible background signal due to the purchased DGH probe containing a few free hemins. These results demonstrated that the developed system could be used as a sensor system with low colorimetric background for visual nucleic acid diagnosis.

The catalytic activity of G16C/hemin DNAzymes was also verified by fluorescence and chemiluminescence assays (Figure S15). The "signal-on" colorimetric assay development and

https://doi.org/10.1021/acssensors.2c01391
ACS Sens. XXXX, XXX, XXX−XXX

Table 1. Comparison of the Proposed Assay with a Commercial qPCR Assay for the Detection of GBS DNA in Real Clinical Specimens

methods		qPCR			compared with qPCR	
		positive	negative	total	sensitivity (%)	specificity (%)
fluorescent strategy	positive	16	0	16	100	100
	negative	0	7	7		
	total	16	7	23		
"signal-on" colorimetric strategy	positive	16	0	16	100	100
	negative	0	7	7		
	total	16	7	23		

optimization involved the stem length, loop length, and concentration of DGH probes; the incubation time of Cas12 for the cleavage of DGH probes; the H_2O_2 concentration for ABTS catalysis; and the catalytic reaction time of ABTS. The optimal parameter combination to enable the best analytical performance is summarized in Figures S16−S22. Under the developed conditions, the "signal-on" colorimetric strategy was used for ultrasensitive detection of GBS DNA. As shown in the inset of Figure 4E, the green color gradually deepened with increasing GBS DNA concentration from 0 to 10^4 pM, and the LOD obtained by the naked eye was 10 pM. In addition, a good correlation was achieved between the absorbance at 414 nm and the GBS DNA concentration from 10^1 to 10^4 pM. The regression equation was expressed as $y = 0.022 + 0.251\lg C_{GBS}$ ($R^2 = 0.988$) (Figure 4E). The LOD obtained by a UV−vis spectrophotometer was 10 pM. Notably, the sensitivity of this approach could be further improved to 1 aM by introducing the RPA technology (Figure 4F inset), which is comparable to the previously reported Cas12a-based colorimetric assay for nucleic acid detection (Table S1). In addition, the specificity experiment was verified by the comparison of the GBS strain and the non-GBS strains (*S. pneumoniae*, *E. coli*, Group A *Streptococcus*, *S. aureus*). As indicated in Figure S23, we can observe an evident signal response toward GBS compared with that toward other non-GBS strains, implying high selectivity of the proposed colorimetric strategy for specifically distinguishing GBS against other nontargets. These results suggested that the developed "signal-on" colorimetric strategy based on G16C/hemin can be used as a promising reporter to eliminate the inherent background of colorimetric probes by simply mixing the DGH probes and G4/hemin signal element.

Analysis of GBS in Clinical Samples by a Label-Free Visible Fluorescent Strategy and a "Signal-On" Colorimetric Strategy. Encouraged by their ultrahigh sensitivity, the developed label-free fluorescent and "signal-on" colorimetric strategies were further extended to detect GBS in 46 clinical vaginal/anal samples of pregnant women [confirmed by the quantitative polymerase chain reaction (qPCR) assay] (Figure 5A). The GBS DNA extracted from clinical samples was pre-amplified with RPA for 30 min and then detected by the developed fluorescent and "signal-on" colorimetric method. The results are summarized in Figure 5B−E. For the fluorescent strategy, green fluorescence markedly reduced when detecting 16 positive samples, while there was no obvious fluorescence change when detecting 7 negative samples (Figure 5B), demonstrating that the sensitivity and specificity of this strategy for the detection of GBS were 100% (Table 1, Figure S24). These results were further confirmed by recording the fluorescence intensity at 487 nm using a fluorescence spectrophotometer (Figure 5C). All detection results were consistent with those of the commercial qPCR assay (Figure S25). For the "signal-on" colorimetric strategy, an obvious green solution was observed when detecting 16 positive samples, while no color change was observed when detecting 7 negative samples (Figure 5D), demonstrating that the sensitivity and specificity of this strategy for the detection of GBS were 100% (Table 1, Figure S26). These results were further confirmed by recording the absorbance at 414 nm using a UV−vis spectrophotometer (Figure 5E). All detection results were also consistent with those of the commercial qPCR assay (Figure S27). In brief, these two strategies could correctly test all negative and positive samples without false-positive and false-negative results, indicating that the developed pre-folded G4-based signal elements could act as a promising next-generation reporter in the CRISPR/Cas12a-based POC testing system.

CONCLUSIONS

We have reported the pre-folded G4 structures with tunable tolerance to CRISPR/Cas12a trans-cleavage and demonstrated their potential as a new signal transduction element in improving CRISPR/Cas12a-based visual nucleic acid diagnosis. By regulating the loop length of the well-folded G4 structure, we systematically explored the relationship between the sensitivity of G4s to CRISPR/Cas12a trans-cleavage and its structure and found that the tolerance was determined by the loop length in G4s. On this basis, two G4 structures, Tel22-10 and G16C, which have high sensitivity and tolerance to CRISPR/Cas12a trans-cleavage, respectively, were designed as fluorescent and "signal-on" colorimetric signal transduction elements to achieve ultrasensitive detection of GBS at the attomolar level. The feasibility of the G4-assisted CRISPR/Cas12a fluorescent and colorimetric strategy in actual clinical diagnosis was well demonstrated. Given its outstanding advantages over the conventional fluorophore quencher-labeled ssDNA reporter and gold nanoparticle ssDNA reporter, the pre-folded G4 structures with tunable tolerance to CRISPR/Cas12a trans-cleavage can serve as a promising signal transduction strategy for the development of ultrasensitive visual POC molecular diagnostics systems.

ASSOCIATED CONTENT

Supporting Information

The Supporting Information is available free of charge at https://pubs.acs.org/doi/10.1021/acssensors.2c01391.

Quantitative analysis of the G4 band intensity in PAGE assay (Figure 1H) by Image J 7.0; tolerance of raw G4 sequence, G4 structures pre-folded by reaction buffer to CRISPR/Cas12a trans-cleavage; tolerance of G16C structure and Tel22 structure to CRISPR/Cas12a trans-cleavage after pre-folded by different concentra-

https://doi.org/10.1021/acssensors.2c01391
ACS Sens. XXXX, XXX, XXX−XXX

tions of K+ and with 100 mM K+ for different times; tolerance of G16C-10 structure and Tel22-10 structure to CRISPR/Cas12a trans-cleavage; comparison of the effect of K+ concentration in the reaction buffer on the trans-cleavage efficiency of Cas12a; comparison of the cleavage efficiency of Cas12a on the unfolded ssDNA sequence and Tel22-10 structure; conditions optimization of "signal-on" colorimetric strategy; specificity detection of the label-free visual fluorescence strategy and "signal-on" colorimetric system; ROC analysis of clinical samples detected by label-free visual fluorescence strategy and "signal-on" colorimetric strategy; qPCR results of GBS in 46 clinical vaginal/anal samples of pregnant women detected by the label-free visual fluorescence or "signal-on" colorimetric assays; comparison between the proposed "signal-on" colorimetric strategy and other reported colorimetric methods based on Cas12a for nucleic acid detection; and DNA sequences employed in this work (PDF)

AUTHOR INFORMATION

Corresponding Authors

Juan Li − *State Key Laboratory of Food Science and Technology, School of Food Science and Technology, Nanchang University, Nanchang 330047, China*; Email: chengwei@hospital.cqmu.edu.cn

Xiaolin Huang − *State Key Laboratory of Food Science and Technology, School of Food Science and Technology, Nanchang University, Nanchang 330047, China*; Email: juanli0905@163.com

Ben Zhong Tang − *School of Science and Engineering, Shenzhen Institute of Aggregate Science and Technology, The Chinese University of Hong Kong, Shenzhen, Guangdong 518172, China*; orcid.org/0000-0002-0293-964X; Email: xiaolin.huang@ncu.edu.cn

Wei Cheng − *The Centre for Clinical Molecular Medical Detection, The First Affiliated Hospital of Chongqing Medical University, Chongqing 400016, China*; orcid.org/0000-0002-1921-9761; Email: tangbenz@cuhk.edu.cn

Authors

Tiantian Yang − *The Centre for Clinical Molecular Medical Detection, The First Affiliated Hospital of Chongqing Medical University, Chongqing 400016, China*

Decai Zhang − *The Centre for Clinical Molecular Medical Detection, The First Affiliated Hospital of Chongqing Medical University, Chongqing 400016, China*; orcid.org/0000-0003-3415-2718

Xiaoxue Cheng − *The Centre for Clinical Molecular Medical Detection, The First Affiliated Hospital of Chongqing Medical University, Chongqing 400016, China*

Jia Li − *The Centre for Clinical Molecular Medical Detection, The First Affiliated Hospital of Chongqing Medical University, Chongqing 400016, China*

Shijia Ding − *Key Laboratory of Clinical Laboratory Diagnostics (Ministry of Education), College of Laboratory Medicine, Chongqing Medical University, Chongqing 400016, China*; orcid.org/0000-0002-9183-1656

Complete contact information is available at: https://pubs.acs.org/10.1021/acssensors.2c01391

Author Contributions

The manuscript was written through contributions of all authors. All authors have given approval to the final version of the manuscript.

Notes

The authors declare no competing financial interest.

ACKNOWLEDGMENTS

This work was funded by the Natural Science Foundation of China (81873972, 81873980, and 32172296), the Foundation for Innovative Research Groups of Chongqing Higher Education Institutions (CXQT20013), the Chongqing Science Fund for Distinguished Young Scholars (cstc2019jcyjjqX0028), and the Chongqing Talents-Innovation Leading Talents Project (CQYC20200303107).

REFERENCES

(1) Chen, J. S.; Ma, E.; Harrington, L. B.; Da Costa, M.; Tian, X.; Palefsky, J. M.; Doudna, J. A. CRISPR-Cas12a target binding unleashes indiscriminate single-stranded DNase activity. *Science* **2018**, *360*, 436−439.

(2) Li, Y.; Li, S.; Wang, J.; Liu, G. CRISPR/Cas systems towards next-generation biosensing. *Trends Biotechnol.* **2019**, *37*, 730−743.

(3) Xiong, Y.; Zhang, J.; Yang, Z.; Mou, Q.; Ma, Y.; Xiong, Y.; Lu, Y. Functional DNA regulated CRISPR-Cas12a sensors for Point-of-Care diagnostics of non-nucleic-acid targets. *J. Am. Chem. Soc.* **2020**, *142*, 207−213.

(4) Hu, M.; Yuan, C.; Tian, T.; Wang, X.; Sun, J.; Xiong, E.; Zhou, X. Single-step, salt-aging-free, and thiol-free freezing construction of AuNP-based bioprobes for advancing CRISPR-based diagnostics. *J. Am. Chem. Soc.* **2020**, *142*, 7506−7513.

(5) Ding, X.; Yin, K.; Li, Z.; Lalla, R. V.; Ballesteros, E.; Sfeir, M. M.; Liu, C. Ultrasensitive and visual detection of SARS-CoV-2 using all-in-one dual CRISPR-Cas12a assay. *Nat. Commun.* **2020**, *11*, 4711.

(6) Xing, S.; Lu, Z.; Huang, Q.; Li, H.; Wang, Y.; Lai, Y.; He, Y.; Deng, M.; Liu, W. An ultrasensitive hybridization chain reaction-amplified CRISPR-Cas12a aptasensor for extracellular vesicle surface protein quantification. *Theranostics* **2020**, *10*, 10262−10273.

(7) Ma, L.; Yin, L.; Li, X.; Chen, S.; Peng, L.; Liu, G.; Ye, S.; Zhang, W.; Man, S. A smartphone-based visual biosensor for CRISPR-Cas powered SARS-CoV-2 diagnostics. *Biosens. Bioelectron.* **2022**, *195*, 113646.

(8) Takahashi, S.; Kotar, A.; Tateishi-Karimata, H.; Bhowmik, S.; Wang, ZF.; Chang, T. C.; Sato, S.; Takenaka, S.; Plavec, J.; Sugimoto, N. Chemical modulation of DNA replication along G-Quadruplex based on topology-dependent ligand binding. *J. Am. Chem. Soc.* **2021**, *143*, 16458−16469.

(9) Miglietta, G.; Russo, M.; Capranico, G. G-quadruplex-R-loop interactions and the mechanism of anticancer G-quadruplex binders. *Nucleic Acids Res.* **2020**, *48*, 11942−11957.

(10) Nishio, M.; Tsukakoshi, K.; Ikebukuro, K. G-quadruplex: Flexible conformational changes by cations, pH, crowding and its applications to biosensing. *Biosens. Bioelectron.* **2021**, *178*, 113030.

(11) Sauer, M.; Paeschke, K. G-quadruplex unwinding helicases and their function in vivo. *Biochem. Soc. Trans.* **2017**, *45*, 1173−1182.

(12) Xu, L.; Liu, S.; Yang, T.; Shen, Y.; Zhang, Y.; Huang, L.; Zhang, L.; Ding, S.; Song, F.; Cheng, W. DNAzyme catalyzed tyramide depositing reaction for in situ imaging of protein status on the cell surface. *Theranostics* **2019**, *9*, 1993−2002.

(13) Meng, H. M.; Hu, X. X.; Kong, G. Z.; Yang, C.; Fu, T.; Li, Z.; Zhang, X. Aptamer-functionalized nanoscale metal-organic frameworks for targeted photodynamic therapy. *Theranostics* **2018**, *8*, 4332−4344.

(14) Khusbu, F. Y.; Zhou, X.; Chen, H.; Ma, C.; Wang, K. Thioflavin T as a fluorescence probe for biosensing applications. *TrAC, Trends Anal. Chem.* **2018**, *109*, 1−18.

(15) Renaud de la Faverie, A.; Guédin, A.; Bedrat, A.; Yatsunyk, L. A.; Mergny, J. L. Thioflavin T as a fluorescence light-up probe for G4 formation. *Nucleic Acids Res.* **2014**, *42*, No. e65.
(16) Jing, S.; Liu, Q.; Jin, Y.; Li, B. Dimeric G-Quadruplex: An effective nucleic acid scaffold for lighting up thioflavin T. *Anal. Chem.* **2021**, *93*, 1333−1341.
(17) Peters, G. M.; Skala, L. P.; Davis, J. T. A molecular chaperone for G4-quartet hydrogels. *J. Am. Chem. Soc.* **2016**, *138*, 134−139.
(18) Zheng, J.; Du, Y.; Wang, H.; Peng, P.; Shi, L.; Li, T. Ultrastable bimolecular G-quadruplexes programmed DNA nanoassemblies for reconfigurable biomimetic DNAzymes. *ACS Nano* **2019**, *13*, 11947−11954.
(19) Li, W.; Li, Y.; Liu, Z.; Lin, B.; Yi, H.; Xu, F.; Nie, Z.; Yao, S. Insight into G-quadruplex-hemin DNAzyme/RNAzyme: adjacent adenine as the intramolecular species for remarkable enhancement of enzymatic activity. *Nucleic Acids Res.* **2016**, *44*, 7373−7384.
(20) He, K.; Sun, L.; Wang, L.; Li, W.; Hu, G.; Ji, X.; Zhang, Y.; Xu, X. Engineering DNA G-quadruplex assembly for label-free detection of Ochratoxin A in colorimetric and fluorescent dual modes. *J. Hazard. Mater.* **2022**, *423*, 126962.
(21) He, L.; Chen, F.; Zhang, D.; Xie, S.; Xu, S.; Wang, Z.; Zhang, L.; Cui, C.; Liu, Y.; Tan, W. Transducing complex biomolecular interactions by temperature-output artificial DNA signaling networks. *J. Am. Chem. Soc.* **2020**, *142*, 14234−14239.
(22) Li, Y.; Li, T.; Liu, BF.; Hu, R.; Zhu, J.; He, T.; Zhou, X.; Li, C.; Yang, Y.; Liu, M. CRISPR-Cas12a trans-cleaves DNA G-quadruplexes. *Chem. Commun.* **2020**, *56*, 12526−12529.
(23) Chen, X.; Wang, L.; He, F.; Chen, G.; Bai, L.; He, K.; Zhang, F.; Xu, X. Label-free colorimetric method for detection of vibrio parahaemolyticus by trimming the G-Quadruplex DNAzyme with CRISPR/Cas12a. *Anal. Chem.* **2021**, *93*, 14300−14306.
(24) Yin, L.; Duan, N.; Chen, S.; Yao, Y.; Liu, J.; Ma, L. Ultrasensitive pathogenic bacteria detection by a smartphone-read g-quadruplex-based CRISPR-Cas12a bioassay. *Sens. Actuators, B* **2021**, *347*, 130586.
(25) Wang, D.; Chen, G.; Lyu, Y.; Feng, E.; Zhu, L.; Pan, C.; Zhang, W.; Liu, X.; Wang, H. A CRISPR/Cas12a-based DNAzyme visualization system for rapid, non-electrically dependent detection of Bacillus anthracis. *Emerging Microbes Infect.* **2022**, *11*, 428−437.
(26) Xia, X.; Ma, B.; Zhang, T.; Lu, Y.; Khan, MR.; Hu, Y.; Lei, C.; Deng, S.; He, Q.; He, G.; Zhang, K.; Deng, R. G-Quadruplex-probing CRISPR-Cas12 assay for label-free analysis of foodborne pathogens and their colonization in vivo. *ACS Sens.* **2021**, *6*, 3295−3302.
(27) Lin, C.; Wu, G.; Wang, K.; Onel, B.; Sakai, S.; Shao, Y.; Yang, D. Molecular recognition of the hybrid-2 human telomeric G-Quadruplex by epiberberine: insights into conversion of telomeric G-quadruplex structures. *Angew. Chem., Int. Ed.* **2018**, *57*, 10888−10893.
(28) Liu, L.; Shao, Y.; Peng, J.; Huang, C.; Liu, H.; Zhang, L. Molecular rotor-based fluorescent probe for selective recognition of hybrid G-quadruplex and as a K^+ sensor. *Anal. Chem.* **2014**, *86*, 1622−1631.
(29) Chen, J.; Guo, Y.; Zhou, J.; Ju, H. The effect of adenine repeats on G-quadruplex/hemin peroxidase mimicking DNAzyme activity. *Chemistry* **2017**, *23*, 4210−4215.
(30) Wang, Z.; Zhao, J.; Bao, J.; Dai, Z. Construction of metal-ion-free G-quadruplex-hemin DNAzyme and its application in S1 nuclease detection. *ACS Appl. Mater. Interfaces* **2016**, *8*, 827−833.
(31) Li, J.; Wu, H.; Yan, Y.; Yuan, T.; Shu, Y.; Gao, X.; Zhang, L.; Li, S.; Ding, S.; Cheng, W. Zippered G-quadruplex/hemin DNAzyme: exceptional catalyst for universal bioanalytical applications. *Nucleic Acids Res.* **2021**, *49*, 13031−13044.
(32) del Villar-Guerra, R.; Trent, J. O.; Chaires, J. B. G-Quadruplex secondary structure obtained from circular dichroism spectroscopy. *Angew. Chem., Int. Ed.* **2018**, *57*, 7171−7175.
(33) Gu, Z.; Fu, A.; Ye, L.; Kuerban, K.; Wang, Y.; Cao, Z. Ultrasensitive chemiluminescence biosensor for nuclease and bacterial determination based on hemin-encapsulated mesoporous silica nanoparticles. *ACS Sens.* **2019**, *4*, 2922−2929.
(34) Xu, F.; Lu, Q.; Huang, P. J.; Liu, J. Nanoceria as a DNase I mimicking nanozyme. *Chem. Commun.* **2019**, *55*, 13215−13218.
(35) Zhou, Z.; Zhu, J.; Zhang, L.; Du, Y.; Dong, S.; Wang, E. G-quadruplex-based fluorescent assay of S1 nuclease activity and K^+. *Anal. Chem.* **2013**, *85*, 2431−2435.
(36) Li, S. Y.; Cheng, Q. X.; Liu, J. K.; Nie, X. Q.; Zhao, G. P.; Wang, J. CRISPR-Cas12a has both cis- and trans-cleavage activities on single-stranded DNA. *Cell Res.* **2018**, *28*, 491−493.
(37) Yuan, R.; Ding, S.; Yan, Y.; Zhang, Y.; Zhang, Y.; Cheng, W. A facile and pragmatic electrochemical biosensing strategy for ultrasensitive detection of DNA in real sample based on defective T junction induced transcription amplification. *Biosens. Bioelectron.* **2016**, *77*, 19−25.
(38) Li, J.; Xiang, Y.; Zhang, L.; Huang, L.; Teng, J.; Ding, S.; Cheng, W. Dynamic DNA self-assembly activated hemin-mimetic enzyme system for versatile fluorescent biosensing. *Sens. Actuators, B* **2019**, *288*, 757−762.
(39) Li, J.; Yuan, T.; Yang, T.; Xu, L.; Zhang, L.; Huang, L.; Cheng, S.; Ding, S. DNA-grafted hemin with preferable catalytic properties than G-quadruplex/hemin for fluorescent miRNA biosensing. *Sens. Actuators, B* **2018**, *271*, 239−246.
(40) Wang, Q.; Xu, N.; Lei, J.; Ju, H. Regulative peroxidase activity of DNA-linked hemin by graphene oxide for fluorescence DNA sensing. *Chem. Commun.* **2014**, *50*, 6714−6717.

Recommended by ACS

Quantum Dot-Based Molecular Beacons for Quantitative Detection of Nucleic Acids with CRISPR/Cas(N) Nucleases
Christopher M. Green, Sebastián A. Díaz, *et al.*
NOVEMBER 15, 2022
ACS NANO
READ

An Ultrasensitive, One-Pot RNA Detection Method Based on Rationally Engineered Cas9 Nickase-Assisted Isothermal Amplification Reaction
Ting Wang, Bang-Ce Ye, *et al.*
AUGUST 31, 2022
ANALYTICAL CHEMISTRY
READ

Integrating CRISPR-Cas12a with a crRNA-Mediated Catalytic Network for the Development of a Modular and Sensitive Aptasensor
Xiaojia Shu, Yurong Yan, *et al.*
AUGUST 10, 2022
ACS SYNTHETIC BIOLOGY
READ

Designing a CRISPR/Cas12a- and Au-Nanobeacon-Based Diagnostic Biosensor Enabling Direct, Rapid, and Sensitive miRNA Detection
Tong Luo, Shian Zhong, *et al.*
APRIL 22, 2022
ANALYTICAL CHEMISTRY
READ

Get More Suggestions >

https://doi.org/10.1021/acssensors.2c01391
ACS Sens. XXXX, XXX, XXX−XXX